

# ChemComm

Accepted Manuscript



This article can be cited before page numbers have been issued, to do this please use: H. Fang, J. Du, C. Tian, J. Zheng, X. Duan, L. Ye and Y. Yuan, *Chem. Commun.*, 2017, DOI: 10.1039/C7CC05487D.



This is an Accepted Manuscript, which has been through the Royal Society of Chemistry peer review process and has been accepted for publication.

Accepted Manuscripts are published online shortly after acceptance, before technical editing, formatting and proof reading. Using this free service, authors can make their results available to the community, in citable form, before we publish the edited article. We will replace this Accepted Manuscript with the edited and formatted Advance Article as soon as it is available.

You can find more information about Accepted Manuscripts in the [author guidelines](#).

Please note that technical editing may introduce minor changes to the text and/or graphics, which may alter content. The journal's standard [Terms & Conditions](#) and the ethical guidelines, outlined in our [author and reviewer resource centre](#), still apply. In no event shall the Royal Society of Chemistry be held responsible for any errors or omissions in this Accepted Manuscript or any consequences arising from the use of any information it contains.



Journal Name

COMMUNICATION

## Regioselective hydrogenolysis of aryl ether C–O bonds by tungsten carbides with controlled phase compositions

Huihuang Fang, Junmou Du, Chenchen Tian, Jianwei Zheng, Xinping Duan, Linmin Ye and Youzhu Yuan\*

Received 00th January 20xx,  
Accepted 00th January 20xx

DOI: 10.1039/x0xx00000x

www.rsc.org/

**Evenly dispersed tungsten carbides with controlled phase compositions that exhibit the impressive capacity to carry out the regioselective hydrogenolysis of inert aryl ether C–O bonds instead of aliphatic C–O bonds to produce aromatic compounds are reported.**

Selective hydrogenolysis of carbon–oxygen (C–O) bonds in aromatic ethers to produce aromatic compounds in a controlled manner is an important and highly desired process particularly because of its connection to the conversion of oxygen-rich lignocellulosic biomass to value-added chemicals and fuels.<sup>1–4</sup> However, this process remains challenging because of the high bond strength and stability of those linkages.<sup>5</sup> Generally, the cleavage of inert aryl C–O bonds requires elevated reaction temperatures and high H<sub>2</sub> pressures. Because competing reactions such as hydrogenation of aromatic rings, hydrogenolysis of aliphatic C–O bonds (with lower bond energy than aryl C–O bonds) can result in poor selectivity, the process usually generates a mixture of products.<sup>1,6–8</sup> Several homogeneous catalysts based on nickel compounds have been reported for efficient hydrogenolysis of aryl C–O bonds,<sup>6,7,9–11</sup> but their availability for large-scale applications is limited. To this end, supported Ni catalysts have been developed and exhibit promising activity for hydrogenolysis of C–O bonds in aromatic ethers such as anisole, guaiacol (GUA) and diphenyl ether.<sup>12–17</sup> However, these catalysts always cause hydrogenation of the aromatic rings, thus increasing the excessive hydrogen consumption and rendering the reaction less meaningful for producing aromatic compounds. Therefore, designing a catalyst for the reaction with sufficiently high selectivity for the target C–O bonds is particularly urgent. Specifically, of particular importance for this required process is to develop efficient catalysts for selective hydrogenolysis of C–O bonds that will not hydrogenate the aromatic rings of aromatic ethers containing varied Ar–OR, Ar–OH, and ArO–R moieties.

State Key Laboratory of Physical Chemistry of Solid Surfaces, National Engineering Laboratory for Green Chemical Productions of Alcohols-Ethers-Esters, iChEM, College of Chemistry and Chemical Engineering, Xiamen University, Xiamen 361005, China. Email: yzyuan@xmu.edu.cn; Fax: +86-592-2183047

\*Electronic Supplementary Information (ESI) available: Supporting figures, tables, and detailed experimental procedures. See DOI: 10.1039/x0xx00000x

Over the past few decades, transition metal carbides have attracted substantial interest as catalytic materials, owing to their noble-metal-like catalytic behaviors, and they have been reported as promising catalysts for a range of important reactions.<sup>18–25</sup> Theoretical calculations have shown that the insertion of carbon into parent transition metals can result in higher d-band electronic density of states at the Fermi level, thus altering the electronic properties and binding energy of the metal and affecting their catalytic performance.<sup>18,26</sup> In particular, tungsten carbides have been investigated and adopted for hydrogenolysis, hydrodeoxygenation, and H<sub>2</sub> evolution reactions, etc.<sup>18–26</sup> The formation of metal carbides, carburization control, and the diffusion of carbon serve the primary catalytic behaviors of metal carbides.<sup>18,26</sup> Multi-walled carbon nanotubes have been employed as solid carbon precursors to alleviate the diffusion rate of carbon atoms, thus allowing for efficient synthesis of phase-pure W<sub>2</sub>C nanoparticles involving impressive H<sub>2</sub> evolution reaction performances.<sup>18</sup> Additionally, tungsten carbides display promising activity for the deoxygenation of oleic acid and stearic acid through cleavage of C–O bonds.<sup>19,20,25</sup> Relatedly, Jongerius *et al.* have investigated the hydrogenolysis of GUA with carbon nanofibers-supported tungsten carbides at 350 °C, obtaining total phenolics [phenol (PhOH) and cresol] selectivity of 58%.<sup>21</sup> Despite these progresses, tungsten carbides in previous reports have always exhibited lower activity than that of molybdenum carbides which are urgent to be improved and there are very few methods to modulate their catalytic performance through controlling the phase composition.<sup>24,27,28</sup>

Motivated by this need, we synthesized a series of tungsten carbide catalysts (W<sub>x</sub>C@CS-*t*, *x*=1, 2; CS and *t* represent carbon spheres and carburizing time, respectively) with different phase compositions by controlling the extent of carburization. Almost quantitative conversion of aromatic ethers and high selectivity to corresponding aromatic compounds were achieved through the hydrogenolysis of inert aryl C–O bonds with the optimized W<sub>x</sub>C@CS-*t* which is probably attributed to the formation of W<sub>x</sub>C by inserting proper amount of carbons.

The W<sub>x</sub>C@CS-*t* catalysts were synthesized according to a previously described procedure with some modifications.<sup>29</sup> The precursor obtained by the polycondensation of resorcinol with formaldehyde was carburized at 850 °C for 1–6 h under H<sub>2</sub>, and then passivated using a 1%O<sub>2</sub>/99%N<sub>2</sub> flow at ambient

ChemComm Accepted Manuscript

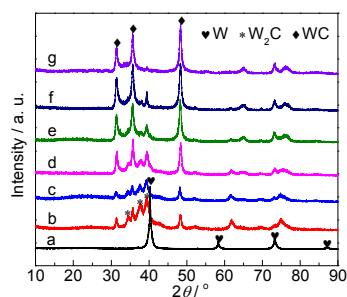


**Fig. 1** XRD patterns of catalysts prepared by different carburization of precursors: (a) W@CS; (b)  $W_xC@CS-1h$ ; (c)  $W_xC@CS-2h$ ; (d)  $W_xC@CS-3h$ ; (e)  $W_xC@CS-4h$ ; (f)  $W_xC@CS-5h$ ; (g)  $W_xC@CS-6h$ .

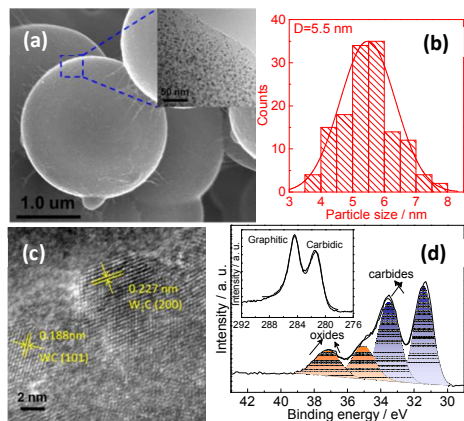


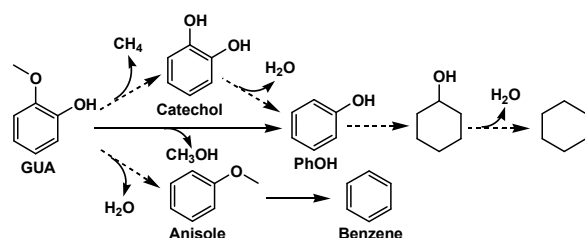
**Fig. 2** (a) SEM and TEM images of  $W_xC@CS-3h$ ; (b) size distribution diagram of  $W_xC@CS-3h$ ; (c) HRTEM image of  $W_xC@CS-3h$ ; (d) W 4f and C 1s XPS profiles of  $W_xC@CS-3h$ .

temperature. For comparison, a catalyst treated at 700 °C for 2 h under  $H_2$  using the same precursor was labeled as W@CS (see Electronic Supplementary Information (ESI) for details for the preparation of all materials). Fig. 1 shows the XRD patterns of catalysts with different carburizing time. Four characteristic diffractions in the W@CS catalyst, centered at  $2\theta$  of 40.42°, 58.36°, 73.33° and 86.91°, were attributed to the metal tungsten phase (Fig. 1a). No peaks of tungsten carbides ( $W_2C$  and WC) were observed. In contrast,  $W_xC@CS-t$  catalysts carburized at 850 °C (Fig. 1b-g) showed completely different diffraction peaks and the phase composition of tungsten carbides varied depending on the carburizing time, which was caused by the increased diffusion time of carbon atoms from the phenolic polymer to the metal tungsten matrix. Well-crystallized  $W_2C$  ( $2\theta = 34.47^\circ, 38.10^\circ, 39.67^\circ, 62.26^\circ$ ) and WC ( $2\theta = 31.70^\circ, 35.89^\circ, 48.65^\circ, 66.23^\circ$ ) were visible in the  $W_xC@CS-1h$  and transformed into phase-pure WC with deeper carburization after 6 h. For the  $W_xC@CS-t$  catalysts,  $N_2$  adsorption revealed that the BET surface area ( $S_{BET}$ ) decreased and finally maintained at approximately  $50 \text{ m}^2 \text{ g}^{-1}$  while the average pore size increased from 3.1 nm to 6.5 nm (Fig. S1 and Table S1). As visualized in Fig. 2a and b, using  $W_xC@CS-3h$  as a representative catalyst, tungsten carbide nanoparticles embedded in uniform large carbon spheres were successfully synthesized. The average nanoparticle diameters are 4–8 nm. The high-resolution TEM (HRTEM) micrograph displayed clear lattice fringes with an interplanar spacing of 0.227 nm and 0.188 nm, corresponding to the (200) of  $W_2C$  and (101) facets

of WC (Fig. 2c). To gain insight into the electronic properties and binding energy of carbide nanoparticles, in situ X-ray photoelectron spectroscopy (in situ XPS) measurements were conducted and the results are shown in Fig. 2d. Two pronounced peaks appeared at 31.7 eV and 33.8 eV corresponding to the typical characteristic peaks of tungsten carbides.<sup>18</sup> Despite  $H_2$  pretreatment before XPS testing, peaks ascribed to the tungsten oxides at 35.4 eV and 37.5 eV, which is owing to the  $O_2$  passivation during preparation, were still visible. In addition, two direct C1s peaks (Fig. 2d, insert) confirmed the presence of graphitic and carbidic carbon species on the outer surface of  $W_xC@CS-t$ .<sup>18,30</sup>

The selective hydrogenolysis of GUA was chosen for initial investigations into the activity of W-based catalysts for hydrogenolysis of C–O bonds because GUA contains methoxyl and hydroxyl functional groups, which forms three types of C–O bonds.<sup>31–34</sup> As shown in Scheme 1, the GUA conversion is a multi-step tandem reaction. The cleavage of weaker aliphatic C–O bond to yield catechol is in competition with cleavage of the inert aryl C–O bond to directly generate PhOH (trace anisole in some cases). Then, PhOH can be easily converted into cyclohexanol and cyclohexane by excessive hydrogenation, thus causing low selectivity.<sup>15</sup> The key element in promoting PhOH selectivity is enhancing the cleavage of aryl C–O bond and suppressing aliphatic C–O bond cleavage and hydrogenation of aromatic ring.

Table 1 shows the catalytic performance of various W-based catalysts for hydrogenolysis of GUA at 300 °C. The PhOH is predominant in the product mixture, demonstrating high selectivity of the  $W_xC@CS-t$  catalysts, whereas only small amounts of anisole and cresols were detected as side-products. No ring-saturated products were observed in this work, thus indicating that tungsten carbide nanoparticles are highly selective for aryl C–O bond cleavage avoiding the occurrence of ring-hydrogenation. Furthermore, as for the  $W_xC@CS-t$  catalysts, the catalytic activity improved as the carburization time increased in terms of both GUA conversion and PhOH selectivity, presumably because of the enhanced insertion of carbon, which affects electronic properties and binding energy. To exclude the effect of porosity, we calculated the diameters of several molecules like GUA, anisole, PhOH, and benzene with GaussView software (Fig. S2). The values were much smaller than the average pore size of  $W_xC@CS-t$  catalysts, indicating that these molecules might be shuttled through the catalyst pores without excessive restraint. The GUA conversion increased from 79.9% to 99.8% with a remarkable enhancement in PhOH selectivity (from 78.6% to 92.7%) when the carburizing time was increased to 3 h. However, further carburization caused a decrease in activity and PhOH selectivity. Apparently,  $W_xC@CS-3h$  exhibited the best catalytic performance for hydrogenolysis of GUA in this work.  $W_xC@CS-6h$ , with phase-pure WC displays 30.1% conversion of GUA with 70.1% selectivity for PhOH, whereas commercial WC showed only negligible activity. Previous reports have shown that  $W_2C$  has less negative Gibbs free energy of  $H_2$  adsorption and higher electronic density of states (DOS) at the Fermi level than WC, thereby resulting in altered properties and higher catalytic performance of metal carbides.<sup>18,35</sup> In the present case, the catalysts with a high content of  $W_2C$  species, such as  $W_xC@CS-1h$  and  $W_xC@CS-2h$ , had an increased tendency to cleave the Ar–OH bond, leading to lower PhOH selectivity and higher anisole selectivity. Thus, tunable carburization, which

**Scheme 1** Reaction pathway for GUA conversion to PhOH.**Table 1** Catalytic performance of W-based catalysts for GUA conversion.

Catalyst	W/W <sub>2</sub> C/WC Ratio /% <sup>c</sup>	Conv. /%	C6 product selec. /%				
			PhOH	Anisole	Cresols	Catechol	Others <sup>d</sup>
W@CS <sup>a</sup>	100/0/0	28.2	30.3	1.2	3.9	56.7	7.9
W <sub>x</sub> C@CS-1h	6/70/24	79.9	78.6	8.9	5.3	0.0	7.2
W <sub>x</sub> C@CS-2h	0/59/41	90.3	80.7	7.8	4.9	0.0	6.0
W <sub>x</sub> C@CS-3h	0/43/57	99.8	92.7	4.9	0.6	0.0	1.8
W <sub>x</sub> C@CS-4h	0/18/82	64.7	83.5	5.4	4.3	0.0	6.4
W <sub>x</sub> C@CS-5h	0/4/96	33.1	73.6	5.0	7.6	0.0	13.8
W <sub>x</sub> C@CS-6h	0/0/100	30.1	70.7	3.7	9.7	0.0	15.9
WC <sup>b</sup>	0/0/100	7.1	51.0	0.6	9.3	2.5	36.6

Reaction conditions: weight liquid hourly space velocity (WLHSV) = 3.0 h<sup>-1</sup>, P (H<sub>2</sub>) = 3.0 MPa, H<sub>2</sub>/GUA molar ratio = 50, T = 300 °C; <sup>a</sup> Synthesized by carburization of precursor at 700 °C for 2 h; <sup>b</sup> Commercial material from Aladdin Inc.; <sup>c</sup> The weight ratio was calculated by XRD Rietveld refinement, see Table S2 for details; <sup>d</sup> Trace veratrole and some other unknown products; see Table S4 for C1 product selectivity.

presumably affects the formation of W<sub>2</sub>C and WC species, is beneficial for efficient hydrogenolysis of inert Ar-OMe and producing a high yield of PhOH.

In comparison, W@CS displayed poor GUA conversion and the main product was catechol, indicating preferential hydrogenolysis of the aliphatic C–O bond with metal tungsten catalysts. To further investigate the hydrogenolysis ability of C–O bonds, anisole, with a single aryl methoxyl group, was evaluated for the W@CS and W<sub>x</sub>C@CS-3h catalysts. The product distributions were significantly different between these two catalysts (Table S3). W<sub>x</sub>C@CS-3h exhibited high selectivity for hydrogenolysis of aryl C–O bond and yield benzene as the major product. In contrast, W@CS was inclined to the cleavage of the weaker aliphatic C–O bond, thus resulting in PhOH as the major product. This result was consistent with the trend in the performance for hydrogenolysis of GUA presented above. Lee et al. have reported similar results with Mo<sub>2</sub>C catalysts and have shown that the stronger aryl C–O bond is preferentially cleaved rather than the weaker aliphatic C–O bond during anisole conversion.<sup>27</sup> Interestingly, methane was also produced during the conversion of GUA and anisole with W<sub>x</sub>C@CS-3h (Tables S1 and S2) although no cracking reaction of C6 compounds occurred in these case. To confirm that the PhOH and benzene are produced from GUA and anisole, respectively, by direct cleavage of the aryl C–O bond, we introduced pure methanol to the reaction under identical reaction conditions. As expected, methane was clearly detected, thus verifying that the formation of methane was mainly due to the further hydrogenolysis of the intermediate product methanol. This result further suggested that the cleavage of aryl C–O bonds

contributes significantly to the production of PhOH and methanol in hydrogenolysis of GUA with W<sub>x</sub>C@CS-*t*.

The dependence of catalytic performance on reaction conditions was investigated by using the optimized W<sub>x</sub>C@CS-3h catalyst. As depicted in Fig. S3, unquestionably, higher temperatures clearly increased the conversion but did not cause significant changes in selectivity. The GUA conversion increased from 1.3% to 98.6% with a slight fluctuation of PhOH selectivity among 89%–92% when the temperature was increased from 225 to 300 °C. The H<sub>2</sub> pressure has only a little influence on the conversion, indicated by the observation that GUA conversion increased from 85.4% to 97.1% with an increase in H<sub>2</sub> pressure from 1.0 to 3.0 MPa (Fig. S4). Notably, ring-saturated products were not observed, regardless of increases in temperature and H<sub>2</sub> pressure. These results indicated that W<sub>x</sub>C@CS-*t* catalysts exhibit benign activation of H<sub>2</sub> and excellent regioselective hydrogenolysis of inert aryl C–O bonds even at high H<sub>2</sub> pressure; a case in which most metal catalysts display competitive hydrogenation of aromatic ring during the cleavage of C–O bonds.<sup>13,15</sup> In addition, the H<sub>2</sub>/GUA ratio was evident in Fig. S5. The W<sub>x</sub>C@CS-3h showed high conversions at low H<sub>2</sub>/GUA ratio (between 30:1 and 80:1), but lower conversion with higher H<sub>2</sub>/GUA ratios. This finding indicated that the activation of both H<sub>2</sub> and GUA on the surface of catalyst is necessary for the cleavage of C–O bonds. Furthermore, there was no apparent effect on the GUA conversion under low WLHSV conditions, while it dramatically decreased with increased WLHSV (Fig. S6). The results also confirmed that substantial contact between the catalyst and substrate is essential for obtaining higher conversions of GUA. The GUA conversion and PhOH selectivity over the W<sub>x</sub>C@CS-3h as a function of time are showed in Fig. S7. The W<sub>x</sub>C@CS-3h maintained high GUA conversion for 330 min but displayed slight drop in activity after 360 min. The PhOH selectivity remained relatively stable and slightly fluctuated at a high constant. The XRD patterns of used catalyst showed diffraction lines similar to the fresh catalyst (Fig. S8) and no obvious peaks ascribed to oxides in bulk phase. However, the XPS profiles indicated there was a slight increase in oxidized species on the catalyst surfaces (Fig. S9). Furthermore, the agglomeration of particle size occurred moderately in the used catalyst as revealed by TEM image (Fig. S10). These results suggested that the slight activity loss is probably due to the particle agglomeration and surface oxidation, as also confirmed by previous reports.<sup>21,22</sup>

**Table 2** Catalytic performance of selective hydrogenolysis of various ethers over the W<sub>x</sub>C@CS-3h.

Ether	T /°C	Conv. /%	C6 product selec. /%					Yield <sup>e</sup> /%
			PhOH	Benzene	Anisole	Cresols	Others	
Diphenyl ether	250	100	100	100	0.0	0.0	0.0	200
Anisole	300	100	0.0	96.0	–	0.0	4.0 <sup>b</sup>	96.0
Phenetole	325	97.1	17.3	71.6	–	3.5	7.6	86.3
Veratrole <sup>a</sup>	325	98.6	10.9	60.1	5.1	0.0	27.0 <sup>c</sup>	78.9
Dimethoxy phenol	350	93.1	86.3	0.6	0.0	1.3	11.8 <sup>d</sup>	80.9

Reaction conditions: WLHSV = 3.0 h<sup>-1</sup>, P (H<sub>2</sub>) = 3.0 MPa, H<sub>2</sub>/Ether molar ratio = 50; <sup>a</sup> H<sub>2</sub>/Ether molar ratio = 90; <sup>b</sup> Cyclohexane; <sup>c</sup> Trace aromatic ring-saturated products and some other unknown products; <sup>d</sup> Trace GUA and some other unknown products; <sup>e</sup> Total yield of PhOH and benzene.

Having identified the catalyst with the best performance for the hydrogenolysis of inert aryl C–O bonds, we also tested the catalytic ability of  $W_xC@CS-3h$  in hydrogenolysis of various aromatic ethers under optimal reaction conditions. The efficient cleavage of aryl C–O bonds is an important process for the manufacturing of value-added aromatic compounds such as PhOH and benzene in good yields, particularly because these are the most abundant linkages in oxygen-rich lignocellulosic biomass.<sup>1,2,36</sup> Table 2 shows the catalytic performance of  $W_xC@CS-3h$  for hydrogenolysis of various aromatic ethers. Diphenyl ether was ultimately converted into benzene and PhOH through direct hydrogenolysis of the aryl C–O bond without other side reactions. Almost full conversion and high selectivity for benzene were achieved when anisole was used as the substrate. Similarly, the reaction with phenetole and veratrole as the substrates showed high conversion and considerable selectivity for benzene as the final product although a small amount of PhOH was detected owing to the hydrogenolysis of the weaker aliphatic C–O bonds. The results of the hydrogenolysis of 2,6-dimethoxyphenol were similar to that of GUA, displaying a 93.3% conversion and 86.3% PhOH selectivity at 350 °C through the cleavage of two aryl Ar–OMe bonds.

In conclusion, the  $W_xC@CS-t$  catalysts with identified phase compositions are successfully synthesized through controlled carburization of the phenolic polymers prepared by polycondensation. Unlike other metal catalysts favoring the saturation of aromatic rings, the optimized  $W_xC@CS-3h$  catalyst shows particularly selective cleavage of aryl C–O bonds even at a high temperature and high  $H_2$  pressure. The  $W_xC@CS-3h$  efficiently catalyzes the hydrogenolysis of Ar–OMe bond in GUA to yield PhOH instead of hydrogenolysis of the weaker aliphatic ArO–Me bonds, preventing the formation of the hydrogenated ring products. This catalyst also exhibits excellent capability for the hydrogenolysis of various aromatic ethers, resulting in a high yield of aromatic compounds such as PhOH and benzene. Therefore, we envision that our findings into the one-pot prepared  $W_xC@CS-t$  may serve as a new approach for the design of active carbide catalysts to demonstrate the importance of the active phases and the mode of carbon insertion by carburization for hydrogenolysis catalysis.

This work was supported by the National Key Research and Development Program of China (2017YFA0206801), the Natural Science Foundation of China (21403178, 91545115, and 21473145), the Program for Innovative Research Team in Chinese Universities (IRT\_14R31), the Fundamental Research Funds for the Central Universities (20720170024 and 20720170026), and the Natural Science Foundation of Fujian Province of China (2017J05027).

## Notes and references

- J. Zakzeski, P. C. A. Bruijninx, A. L. Jongerius and B. M. Weckhuysen, *Chem. Rev.*, 2010, 110, 3552.
- J. C. Serrano-Ruiz and J. A. Dumesic, *Energy Environ. Sci.*, 2011, 4, 83.
- A. J. Ragauskas, G. T. Beckham, M. J. Biddy, R. Chandra, F. Chen, M. F. Davis, B. H. Davison, R. A. Dixon, P. Gilna, M. Keller, P. Langan, A. K. Naskar, J. N. Saddler, T. J. Tschaplinski, G. A. Tuskan and C. E. Wyman, *Science*, 2014, 344, 709.

- C. Z. Li, X. C. Zhao, A. Q. Wang, G. W. Huber and T. Zhang, *Chem. Rev.*, 2015, 115, 11559.
- E. Furimsky, *Appl. Catal. A: Gen.*, 2000, 199, 147.
- A. G. Sergeev, J. F. Hartwig, *Science*, 2011, 332, 439.
- Y. L. Ren, M. J. Yan, J. J. Wang, Z. C. Zhang, K. S. Yao, *Angew. Chem. Int. Ed.*, 2013, 52, 12674.
- M. Wang, H. Shi, D. M. Camaioni, J. A. Lercher, *Angew. Chem. Int. Ed.*, 2017, 56, 2110.
- P. Alvarez-Bercedo, R. Martin, *J. Am. Chem. Soc.*, 2010, 132, 17352.
- S. Kusumoto, K. Nozaki, *Nat. Commun.*, 2015, 6, 6296.
- H. J. Xu, B. Yu, H. Y. Zhang, Y. F. Zhao, Z. Z. Yang, J. L. Xu, B. X. Han and Z. M. Liu, *Chem. Commun.*, 2015, 51, 12212.
- J. He, C. Zhao, J. A. Lercher, *J. Am. Chem. Soc.*, 2012, 134, 20768.
- W. Schutyser, S. V. dan Bosch, J. Dijkmans, S. Turner, M. Meledina, G. V. Tendeloo, D. P. Debecker, B. F. Sels, *ChemSusChem*, 2015, 8, 1805.
- W. J. Song, Y. S. Liu, E. Barath, C. Zhao, J. A. Lercher, *Green Chem.*, 2015, 17, 1204.
- H. H. Fang, J. W. Zheng, X. L. Luo, J. M. Du, A. Roldan, S. Leoni and Y. Z. Yuan, *Appl. Catal. A: Gen.*, 2017, 529, 20.
- M. Zaheer, R. Kempe, *ACS Catal.*, 2015, 5, 1675.
- M. Zaheer, J. Hermannsdorfer, W. P. Kretschmer, Günter Motz, and R. Kempe, *ChemCatChem*, 2014, 6, 91.
- Q. F. Gong, Y. Wang, Q. Hu, J. G. Zhou, R. F. Feng, P. N. Duchesne, P. Zhang, F. J. Chen, N. Han, Y. F. Li, C. H. Jin, Y. G. Li and S. T. Lee, *Nat. Commun.*, 2016, 7, 13216.
- R. W. Gosselink, D. R. Stellwagen and J. H. Bitter, *Angew. Chem. Int. Ed.*, 2013, 52, 5089.
- S. A. W. Hollak, R. W. Gosselink, D. S. van Es and J. H. Bitter, *ACS Catal.*, 2013, 3, 2837.
- A. L. Jongerius, R. W. Gosselink, J. Dijkstra, J. H. Bitter, P. C. A. Bruijninx and B. M. Weckhuysen, *ChemCatChem*, 2013, 5, 2964.
- C. Z. Li, M. Y. Zheng, A. Q. Wang and T. Zhang, *Energy Environ. Sci.*, 2012, 5, 6383.
- R. Ma, K. Cui, L. Yang, X. L. Ma and Y. D. Li, *Chem. Commun.*, 2015, 51, 10299.
- C. J. Chen, W. S. Lee and A. Bhan, *Appl. Catal. A: Gen.*, 2016, 510, 42.
- A. Villa, S. Campisi, C. Giordano, K. Otte and L. Prati, *ACS Catal.*, 2012, 2, 1377.
- J. G. Chen, *Chem. Rev.*, 1996, 96, 1477.
- W. S. Lee, Z. S. Wang, R. J. Wu, A. Bhan, *J. Catal.*, 2014, 319, 44.
- M. M. Sullivan, C. J. Chen and A. Bhan, *Catal. Sci. Technol.*, 2016, 6, 602.
- S. Han, D. H. Youn, M. H. Lee and J. S. Lee, *ChemCatChem*, 2015, 7, 1483.
- X. F. Yang, Y. C. Kimmel, J. Fu, B. E. Koel, J. G. Chen, *ACS Catal.*, 2012, 2, 765.
- Y. K. Hong, D. W. Lee, H. J. Eom and K. Y. Lee, *Appl. Catal. B: Environ.*, 2014, 150–151, 438.
- S. K. Wu, P. C. Lai, Y. C. Lin, H. P. Wan, H. T. Lee and Y. H. Chang, *ACS Sustain. Chem. Eng.*, 2013, 1, 349.
- Y. C. Lin, C. L. Li, H. P. Wan, H. T. Lee, C. F. Liu, *Energy & Fuels*, 2011, 25, 890.
- J. M. Sun, A. M. Karim, H. Zhang, L. Kovarik, X. H. S. Li, A. J. Hensley, J. S. McEwen, Y. Wang, *J. Catal.*, 2013, 306, 47.
- J. R. Kitchin, J. K. Nørskov, M. A. Barteau, J. G. Chen, *Catal. Today*, 2005, 105, 66.
- M. Saidi, F. Samimi, D. Karimipourfard, T. Nimmanwudipong, B. C. Gates, M. R. Rahimpour, *Energy Environ. Sci.*, 2014, 7, 103.